



UNIVERSITY OF LEEDS

This is a repository copy of *Ultrasound-mediated gene transfer (sonoporation) in fibrin-based matrices: potential for use in tissue regeneration*.

White Rose Research Online URL for this paper:
<http://eprints.whiterose.ac.uk/96177/>

Version: Accepted Version

Article:

Feichtinger, G (2016) Ultrasound-mediated gene transfer (sonoporation) in fibrin-based matrices: potential for use in tissue regeneration. *Journal of Tissue Engineering and Regenerative Medicine*, 10 (1). pp. 29-39. ISSN 1932-6254

<https://doi.org/10.1002/term.1730>

© 2013 John Wiley & Sons, Ltd. This is the peer reviewed version of the following article: Nomikou, N., Feichtinger, G. A., Redl, H., and McHale, A. P. (2016) Ultrasound-mediated gene transfer (sonoporation) in fibrin-based matrices: potential for use in tissue regeneration. *J Tissue Eng Regen Med*, 10: 29–39; which has been published in final form at <https://dx.doi.org/10.1002/term.1730>. This article may be used for non-commercial purposes in accordance with the Wiley Terms and Conditions for Self-Archiving.

Reuse

Unless indicated otherwise, fulltext items are protected by copyright with all rights reserved. The copyright exception in section 29 of the Copyright, Designs and Patents Act 1988 allows the making of a single copy solely for the purpose of non-commercial research or private study within the limits of fair dealing. The publisher or other rights-holder may allow further reproduction and re-use of this version - refer to the White Rose Research Online record for this item. Where records identify the publisher as the copyright holder, users can verify any specific terms of use on the publisher's website.

Takedown

If you consider content in White Rose Research Online to be in breach of UK law, please notify us by emailing eprints@whiterose.ac.uk including the URL of the record and the reason for the withdrawal request.



eprints@whiterose.ac.uk
<https://eprints.whiterose.ac.uk/>

Ultrasound-mediated gene transfer (sonoporation) in fibrin-based matrices: potential for use in tissue regeneration

Nikolitsa Nomikou¹, Georg A. Feichtinger², Heinz Redl² and Anthony P. McHale^{3*}

¹Sonidel Ltd, Dublin, Ireland

²Ludwig Boltzmann Institute for Experimental and Clinical Traumatology, AUVA Research Centre, Austrian Cluster for Tissue Regeneration, Vienna, Austria

³Department of Pharmacy and Pharmaceutical Sciences, University of Ulster, Northern Ireland

Abstract

It has been suggested that gene transfer into donor cells is an efficient and practical means of locally supplying requisite growth factors for applications in tissue regeneration. Here we describe, for the first time, an ultrasound-mediated system that can non-invasively facilitate gene transfer into cells entrapped within fibrin-based matrices. Since ultrasound-mediated gene transfer is enhanced using microbubbles, we compared the efficacy of neutral and cationic forms of these reagents on the ultrasound-stimulated gene transfer process in gel matrices. In doing so we demonstrated the beneficial effects associated with the use of cationic microbubble preparations that interact directly with cells and nucleic acid within matrices. In some cases, gene expression was increased two-fold in gel matrices when cationic microbubbles were compared with neutral microbubbles. In addition, incorporating collagen into fibrin gels yielded a 25-fold increase in gene expression after application of ultrasound to microbubble-containing matrices. We suggest that this novel system may facilitate non-invasive temporal and spatial control of gene transfer in gel-based matrices for the purposes of tissue regeneration.

Keywords: sonoporation; tissue engineering; gene transfer; microbubbles; fibrin; collagen

1. Introduction

Technologies developed in the field of tissue regeneration employ autologous stem cells in combination with biodegradable scaffold materials in order to successfully and reproducibly restore the function of damaged tissues, including bone, cartilage and vascular tissues. More particularly, developing strategies aimed at stimulating the body to regenerate tissues wherever possible have received considerable attention. Many of the more recent efforts in this area have focused on the use of scaffold materials that emit biochemical signals, such as growth factors, in order to stimulate cellular differentiation (Park et al., 2011) and/or the genetic transformation of cells that can trigger the formation of a specific type of tissue at the site of the defect (Zhao et al., 2005; Kofron and Laurencin, 2006). To date, the approach of employing genetically transformed cells for tissue regeneration has been limited to the use of cells that have been transfected in vitro prior to implantation in ex vivo approaches. This means that the cells must be subjected to prolonged culture in vitro under conditions that do not resemble their true in vivo environments. An alternative approach is to perform the gene transfer event while these cells are housed in 3D matrices that mimic the natural extracellular matrix (ECM), and from this perspective efforts have primarily focused on the use of gene-activated matrices (GAMs). GAMs are matrices that use biocompatible materials and, in addition to serving as tissue scaffolds, are functionalized or possess intrinsic features to facilitate gene transfer to the endogenous or exogenous stem cells that are incorporated into those matrices. Thus far, satisfactory results have been achieved in vivo using collagen matrices activated with adenoviral vectors for induction of vascularization or for optic nerve injury treatment (Gonzalez et al., 2009). The adenoviral vector-based GAMs that offer

potential to be applied in humans have, until now, been limited to those inducing angiogenesis (Mulder et al., 2009). Despite such successes, the risk of immunogenicity elicited by the use of adenovirus and other complications associated with the use of viral vectors in general render this approach suboptimal (Bouuaert and Chalmers, 2009; Bushman, 2007). In efforts to preclude the challenges associated with the use of viral vectors, a variety of alternative gene transfer modalities are emerging. The use of GAMs based on naked plasmid DNA incorporated into collagen matrices to enhance osteogenesis and angiogenesis in segmental bone defects has appeared to offer some advantage; however, effects on bone formation have been variable (Geiger et al., 2005). In general, the use of naked DNA or polymer-protected DNA (Schillinger et al., 2008) in GAMs has appeared to have very low efficacy and efforts to overcome these challenges are ongoing. It should be noted, however, that in addition to the challenges presented by existing viral or non-viral gene transfer methods, all preclude any design aspect that affords extracorporeal, non-invasive spatial control of gene transfer events.

Undoubtedly, an ideal option would be to develop a non-invasive method, which would allow actively induced and targeted gene transfer within the cell-hosting matrices postimplantation. In practical research or clinical applications, such a system would enable non-invasive spatial control of tissue differentiation/development, and this would, in turn, provide the ability to form the desired tissue architecture during tissue regeneration (i.e. site-specific stimulation of blood vessel growth in new replacement tissues). In order to achieve this, one would require a gene transfer stimulus that is noninvasive, would preclude the addition of toxic or immunogenic agents, would not disrupt the matrix and could be applied to a single point in three dimensions with a high degree of precision. Sonoporation, or the use of ultrasound to induce transient cell membrane permeabilization, is emerging as a promising physical, non-viral method for gene transfer (Li et

al., 2009; Nomikou and McHale, 2010). As a stimulus for gene transfer, it appears to harbour all the requisite attributes outlined above as an ideal gene transfer system for use in GAMs, since it is non-invasive, does not involve the use of toxic or immunogenic exogenous agents, would not disrupt a matrix and may be directed to a single point in space with a high degree of spatial control (Li et al., 2009; ter Haar, 2007). This physical method employs ultrasound in combination with microbubbles in order to facilitate cell membrane permeabilization through ultrasound-induced cavitation effects in the microenvironment of the target cells. This enables efficient DNA uptake through the formation of cavitation-induced pores in the cellular membrane. It has previously been shown that this approach can be used to noninvasively stimulate gene transfer into tissues in vivo (Li et al., 2009; Nomikou et al., 2012). From a tissue regeneration perspective, it has also been employed to non-invasively facilitate gene transfer for the purposes of bone healing and regeneration in vivo (Osawa et al., 2009); in that study, the ectopic formation of mature bone in mouse skeletal muscle tissues that were sonoporated with a plasmid encoding human BMP-2 was demonstrated. However, in that study, the authors did not employ exogenously added matrices, a prerequisite for tissue regeneration protocols designed to facilitate orthotopic deficit repair by providing both a pre-formed scaffold to limit gene transfer to the defect site and an architectural template.

The use of matrix or scaffold materials in tissue regeneration offers significant advantages, including enhancing the viability and proliferation of incorporated stem cell populations and promoting their differentiation (Pérez et al., 2013; Keibl et al., 2011). Because they can be applied to and moulded into tissue deficits, they can also provide architectural integrity to the regenerating tissues, retain the incorporated stem cell population in the wound or deficit area and, finally, may serve as a suitable environment for ingress of endogenous stem cells populations (Pérez et al.,

2013). Both collagen and fibrin are amongst the most commonly employed biopolymers for the transplantation of stem cells and have been used as 3D scaffold materials for a wide variety of tissue-engineering applications (Schneider et al., 2010; Schillinger et al., 2008; Feichtinger et al., 2010) . Combined with the appropriate growth or differentiation signals, both materials have been used to promote the desired proliferation and differentiation of stem cells (Liu et al., 2006; Wang et al., 2011).

In this study we decided to determine whether or not ultrasound might provide a means of non-invasively stimulating gene transfer in three-dimensional (3D) matrices. We describe a system compatible with in situ ultrasound-mediated gene transfer into target cells preseeded into 3D fibrin-based matrices. Both neutral and biotinylated cationic microbubbles were examined for their performance in promoting in situ ultrasound-mediated gene transfer to cellular targets in the fibrin-based matrices. In addition, the influence of collagen on ultrasound-mediated gene transfer in these fibrin-based matrices, and the potential use of this system in facilitating temporally and spatially-controlled gene transfer/expression in the field of tissue engineering, are described.

2. Materials and methods

2.1. Plasmid DNA and cell culture

The reporter plasmid pCMV-Luc, encoding the firefly luciferase gene under the control of the CMV promoter, was supplied by PlasmidFactory GmbH & Co (Germany). C2C12 mouse myoblast precursor cells were obtained from in-house stocks and used as an in vitro target for gene transfer and expression in our 3D matrices. Although this cell line is a myoblastic precursor and

differentiates to skeletal muscle by default *in vitro*, it has also been shown to be capable of robust osteogenic differentiation and represents a well-established tool for osteogenic differentiation pathways (Katagiri et al., 1994; Lee et al., 2003; Nakashima et al., 2005). As such, we felt that it was an ideal model candidate to probe ultrasound-mediated gene transfer in 3D matrices. The cell line was maintained in high glucose-containing tissue culture medium (Dulbecco's modified Eagle's medium; DMEM) supplemented with glutamine (GibcoBRL,UK) and 5% v/v fetal bovine serum at 37 C in a 5% CO₂ humidified atmosphere. When required, single cell suspensions were prepared by treating cell monolayers with a 0.05% w/v solution of trypsin containing 0.02% w/v EDTA in phosphate-buffered saline (PBS). Cells were subsequently harvested and washed in Opti-MEM reduced serum medium by centrifugation prior to use.

2.2. Microbubbles

Microbubble reagents were provided by Sonidel Ltd (Ireland). In these studies, two microbubble preparations were employed as sonoporation aids with neutral (SDM201) and biotinylated cationic (SDM302) lipid-based shells (Nomikou et al., 2012). Microbubble suspensions were diluted in PBS when necessary.

2.3. Preparation of the 3D cell-containing matrices for sonoporation

A 25 ml aliquot of cell suspension in Opti-MEM was mixed with 15 ml microbubble suspension. After approximately 4 min, a 10 ml aliquot of DNA solution in Opti-MEM was added to the mixture and this was incubated for a further 5 min. A 25 ml sample of collagen solution (DM1, atelo type I bovine dermal, 3 mg/ml; DevroMedical, UK), neutralized with a 0.4 M phosphate buffer, pH 11.2, was then added to the mixture, followed by the addition of 50 ml Tissucol^W

(Baxter, Austria) containing fibrinogen (110 mg/ml) and aprotinin (3000 KIU/ml) and supplemented with 10% v/v 5 Opti-MEM. A 40 ml aliquot of the final mixture was dispensed into each well of a 96-well plate and mixed with 40 ml thrombin (Tissucol^W Kit, Baxter) solution (25 IU/ml) in CaCl₂ (40 mM), supplemented with 50% v/v 5 Opti-MEM. The mixture solidified and formed a firm gel within 10–15 s at room temperature. Unless otherwise stated, each matrix in the well of a 96-well plate contained 6×10^4 cells, together with microbubbles at a concentration of 4.8×10^7 microbubbles/ml and plasmid DNA at a concentration of 20 mg/ml. This particular cell concentration was chosen in order to maximize contact between the microbubbles and the cells within the gel matrices, and the DNA concentration was chosen because it was previously shown to function optimally in vivo (Li et al., 2009). For matrices in the absence of collagen, the latter was replaced by 25 ml PBS. For matrices in the absence of microbubbles and DNA, the suspension/solution was replaced by PBS and Opti-MEM, respectively. In order to measure the ultrasound permeability of matrices in the presence and the absence of collagen, matrices of 5 mm thickness were prepared and the ultrasound passing through these matrices was measured using an ultrasound power meter (UPM-DT-1 and 10A, OHMIC Instruments, USA), as recommended by the manufacturer.

2.4. Ultrasound-mediated gene transfer and expression

After each fibrin-based matrix had gelled, each well was treated with ultrasound, as described previously (Nomikou et al., 2012), using an SP100 sonoprotator (Sonidel) emitting ultrasound at a frequency of 1 MHz. The transducer had an effective radiating area of 0.8 cm^2 . Samples were treated for 30 s at various ultrasound intensities/power densities, using a 25% duty cycle (pulse frequency 100 Hz). Unless otherwise stated, ultrasound was used at a power density of 4 W/cm^2

(spatial average:temporal peak; SATP). Following ultrasound treatment, a 150 ml aliquot of Opti-MEM was added to each well and the plates were placed in a humidified 5% CO₂ atmosphere at 37 C for 1 h. The Opti-MEM in the well was then replaced by high glucose-containing DMEM supplemented with glutamine (GibcoBRL, UK) and 5% v/v fetal bovine serum and plates were then incubated for 24 h at 37 C in a humidified 5% CO₂ atmosphere, prior to analysis for gene expression. Bioluminescent imaging was used to measure expression of the plasmid-encoded luciferase gene, as this is routinely employed to detect and quantify gene transfer in vitro and in vivo (Nomikou et al., 2012; Li et al., 2009; Correa de Sampaio et al., 2012). The growth medium overlaying the 3D matrices was removed from each well and this was replaced with 50 ml D-luciferin (Biosynth, Switzerland) solution (10 mg/ml solution in serum-free DMEM). The emitted bioluminescence was recorded after 20 min, using a Xenogen IVIS^W Lumina imaging system supported by Living Image^W software v. 2.60. Using this software, each well was marked as a region of interest (ROI) and luciferase activity was expressed as photons emitted/s from each well. For the substrate diffusion studies, the emitted bioluminescent signal was measured every 5 min over a total duration of 40 min.

2.5. Cell viability in 3D matrices

Viability of cells in the 3D matrices was determined using a modification of the method described by Powell et al. (2011) and was based on the cleavage of fluorescein diacetate (Fda) by viable cells. Essentially, culture medium overlaying the matrices was removed from the wells and this was replaced by 50 ml Fda solution in PBS (13 mg/ml). Plates were protected from direct light and incubated at 37 C for a period of 20 min. The fluorescence intensity exhibited by each matrix was measured (from the bottom) using a FLUOstar Omega microplate reader (BMG Labtech,

Germany), at an excitation wavelength of 485 nm and an emission wavelength of 520 nm. Matrices in the absence of cells were used as the zero reference in each case. Cell viability was determined by comparison with a standard curve, constructed using fluorescence intensities from known concentrations of cells in fibrin-based matrices. Since this protocol was non-destructive, repeated measurement of cell viability was possible and, when this was required, matrices in each well were washed twice under sterile conditions with medium (30 min/rinse) and could be re-incubated in a humidified 5% CO₂ atmosphere at 37 C for further analysis.

2.6. Microscopy and histological examination of matrices

In order to observe the interaction of microbubbles with cells within the 3D matrices, 40 ml aliquots of the matrix mixture were placed on a microscope slide and immediately covered with a cover slip. After matrix gelation, samples were observed using a Nikon Eclipse E400 fluorescence microscope (Japan), fitted with a 60 oilimmersion objective. Photomicrographs were acquired using a digital camera interfaced with a PC operating the iQ Standard Video-Meteor II software system v. 1.3 (Andor™ Technology plc, UK).

For histological analyses, matrices were fixed by immersion in 4% paraformaldehyde for 24 h, followed by immersion in 30% w/v sucrose in PBS for another 24 h. Fixed matrices were frozen directly in optimal cutting temperature compound (OCT) embedding medium at 25 C; 45 mm sections were harvested using a CM 1850 cryostat (Leica) and placed in a cryoprotectant solution containing 30% v/v ethylene glycol, 25% v/v glycerol and 45% v/v PBS. The sections were washed with PBS and then placed on poly-L-lysinecoated microscope slides (Fisher, UK). The slides were dried at room temperature overnight. The sections were mounted with 4,6-diamidino-2-phenylindole (DAPI)-containing UltraCruz™ Mounting Medium (Santa Cruz, USA), using

Vectashield mounting medium (Vector Laboratories, UK), as indicated by the manufacturer, in order to determine the number of cell nuclei in a given field. Alternatively, sections were stained for collagen fibres with Weigert's iron haematoxylin and subsequently with Van Gieson's stain. Essentially, the sections were stained with Weigert's iron haematoxylin for 15 min and subsequently washed with running water for a further 15 min. Following rinsing with distilled water, the sections were placed in Van Gieson's stain (saturated aqueous solution of picric acid and 1% w/v acid fuchsin in a 20:1 v/v ratio) for 5 min. The sections were washed with distilled water, rapidly rinsed in 70% v/v ethyl alcohol and then dehydrated rapidly in absolute alcohol. DAPI-stained sections were examined using a multiphoton confocal laser scanning microscope (Leica TCS SP5, Milton Keynes, UK) at excitation and emission wavelengths of 360 nm and 460 nm, respectively. Sections stained for the visualization of collagen were viewed with a Nikon Eclipse E400 fluorescence microscope (Japan), fitted with a 20 objective. Photomicrographs were acquired using a digital camera interfaced with a PC operating the iQ Standard Video-Meteor II software system, v. 1.3 (Andor™Technology).

2.7. Statistical analysis

Statistical analysis of significance was conducted using ANOVA and data groups were compared with the Tukey multiple comparison test (MCT), using GraphPad Prism 4.0. Unless stated otherwise, $p < 0.05$ was considered to indicate statistical significance.

3. Results and discussion

3.1. Effect of ultrasound power density on sonoporation in fibrin–collagen-based matrices

Although a considerable number of studies have resulted in the development of different methods, either chemical or biological, for in situ gene transfer into cells within 3D matrices, no report has described a system that can provide non-invasive spatial and temporal control of gene transfer within those matrices. In order to determine whether or not ultrasound might provide such a stimulus, we used fibrin–collagen-based matrices, containing ultrasoundresponsive microbubbles and plasmid DNA, in order to deliver nucleic acid into C2C12 cells seeded within these matrices. Our rationale for choosing this cell line is described above. In these studies it was also decided to compare neutral microbubbles with a cationic microbubble in gel formulations, since it was previously demonstrated that the latter provided advantage in terms of enhancing ultrasound-mediated gene transfer in vitro and in vivo (Nomikou et al., 2012). Indeed in the latter study, when neutral, cationic and biotinylated cationic microbubbles were compared, it was found that the biotinylated cationic microbubble promoted ultrasound-mediated gene transfer with the greatest efficiency. Therefore, in the current study both neutral (SDM201) and biotinylated cationic (SDM302) microbubbles were compared for their ability to promote ultrasound-mediated gene transfer in the 3D matrices. Each matrix was treated with ultrasound at the indicated power densities in the range 0–5 W/cm²; 24 h after treatment, the 96-well plates were examined using photonic imaging to detect expression of the transgene-encoded luciferase within the cell-containing matrices. The results are shown in Figure 1A and demonstrate that gene expression using both microbubbles increased to an ultrasound power density of 4 W/cm². In the absence of microbubbles, no gene expression was observed at any of the ultrasound intensities examined.

From our previous studies it was interesting to note that optimal gene expression was obtained at ultrasound power densities of 1.3–2 W/cm², using a monolayer in two dimensional (2D) cell culture (Nomikou et al., 2012; Li et al., 2008). At these lower ultrasound power densities, using microbubbles, the levels of gene expression were significantly decreased in the 3D matrices and it was most likely that this was due to attenuation of ultrasound by the gel matrix. It has been shown that optimizing ultrasound-mediated gene transfer, as with any other physical gene transfer modality, involves achieving a compromise between cell viability and gene expression (Nomikou et al., 2012; Suzuki et al., 2011). Indeed, this was confirmed to some degree when the viability of cells within treated matrices was examined; those data are shown in Figure 1B, and demonstrated that, up to ultrasound intensities of 4 W/cm², decreasing cell viability correlated with an increase in gene transfer. However, at 5 W/cm², whilst the cell viability decreased to 50%, gene expression was reduced almost 10-fold when the neutral microbubble was employed (Figure 1A, B). This could suggest that at higher ultrasound power densities, cells that would have expressed the transgene are in some way placed at a survival disadvantage, possibly by an inability to adequately repair the cell membrane following sonoporation. It is clear that this phenomenon was not as dramatic with the cationic microbubble and the decrease in gene expression was not quite as dramatic at 5 W/cm². Interestingly, treatment with ultrasound, in the absence of microbubbles, did not have any significant impact on cell viability at any applied ultrasound intensity up to 5 W/cm². It has previously been demonstrated that ultrasound at a power density of 4 W/cm² (albeit with longer treatment times) in the absence of microbubbles had a significant effect on cell viability when applied to cellular targets in 2D cell culture systems (Li et al., 2008), and again suggests that this may be due to attenuation of the ultrasound stimulus by the matrix. An alternative explanation

for this observation could be that cells in the 3D matrices are protected by those matrices, whereas those in 2D systems are more amenable to destruction because they are in contact with a rigid, non-flexible plastic surface.

In directly comparing the ability of both microbubbles to enhance ultrasound-mediated gene transfer in the 3D matrices, whilst optimal gene expression was observed at an ultrasound power density of 4 W/cm^2 , luciferase gene expression levels were higher when the biotinylated cationic microbubbles were employed (Figure 1A). As mentioned above, it has previously been demonstrated that proximity between microbubbles, nucleic acid and target cells is essential in order for the former to promote sonoporation events (Nomikou et al., 2012; Judo et al., 2009). In applying the use of microbubbles to promote ultrasound-mediated gene transfer in 3D matrices, one might expect the lack of mobility of microbubbles and target cells within the matrix to compromise proximity and therefore negatively influence the efficiency of gene transfer. However, it has also been demonstrated that the biotinylated cationic microbubbles used in this study are extremely efficient at binding both cells and nucleic acid (Nomikou et al., 2012), and such attributes make this reagent ideally suited to use in a gel-based matrix, because it can promote direct interactions between target cells and nucleic acid prior to the formation of the 3D matrix. It is clear from the data in Figure 2 that the biotinylated cationic microbubbles are interacting directly with cells in the matrix, and we suggest that this phenomenon is responsible for the enhanced gene expression observed in Figure 1A, using this microbubble preparation. This is an important design aspect of the system and will be discussed further below.

3.2. Effect of microbubble and DNA concentration on sonoporation in fibrin– collagen-based matrices

Since formulation of the 3D matrix necessitates incorporation of microbubbles and nucleic acid in order to facilitate ultrasound-mediated gene transfer in situ, it was of interest to determine the effect of the concentrations of each of these components on ultrasound-mediated gene transfer. To this end, cells were incorporated into each fibrin–collagen matrix, containing either the pCMV-Luc plasmid together with each microbubble (SDM201 and SDM302) at concentrations of 0– 4.8×10^7 microbubbles/ml or 4.8×10^7 microbubbles/ml, with different plasmid concentrations in the range 0–20 mg/ml. Each matrix was treated at an ultrasound intensity of 4 W/cm^2 . The samples were examined 24 h after treatment, using bioluminescent imaging following addition of luciferin in order to detect expression of the transgene-encoded product luciferase within the cell-containing matrices. The cell viability in each system was also determined. The results presented in Figure 1C, E, demonstrate that the level of luciferase expression in the matrices was dependent on the concentration of microbubbles and the concentration of plasmid employed. More particularly, microbubbles significantly enhanced sonoporation at the highest concentration tested, with use of the biotinylated cationic microbubble providing the highest gene expression levels ($p < 0.001$ when compared with all other groups; Figure 1C). Viability of the sonoporated cells in the matrices decreased with the increasing concentration of microbubbles (Figure 1D), a phenomenon that has previously been reported in systems where cells were treated in 2D culture (Nomikou et al., 2012). It was interesting to note that the neutral microbubble had less of an effect on cell viability at lower microbubble concentrations, and this was probably due to a decreased association between those microbubbles and target cells in the matrix at lower microbubble concentrations. Gene expression levels also increased with increasing plasmid concentration in the 3D system. At the highest DNA

concentration, no gene expression was detected in samples containing DNA and microbubbles in the absence of ultrasound treatment or treated with ultrasound in the absence of microbubbles. As expected, the use of the biotinylated cationic microbubble reagent resulted in higher bioluminescent signals than those obtained using the neutral microbubbles at DNA concentrations of 10 and 20 mg/ml (when comparing neutral with cationic microbubbles; $p < 0.001$; Figure 1E). This result is possibly due to the ability of the biotinylated cationic microbubble to retain plasmid DNA on its surface and in close proximity to the cells (Nomikou et al., 2012). This is confirmed by close examination of the differences in gene expression observed for both microbubbles at a DNA concentration of 10 mg/ml. At this lower concentration of DNA, gene expression obtained with the biotinylated cationic microbubble is almost double that obtained with the neutral microbubble. At this lower DNA concentration, and because the biotinylated cationic microbubble can interact directly with DNA and cells, proximity between DNA and target cells would be expected to be higher than that achieved with the neutral microbubble. It should be mentioned that over the plasmid concentration range used in this part of the study, no significant effect on cell viability was noted.

3.3. Effect of microbubble surface character on the spatial distribution of gene expression in matrices

From the above experiments, it was evident that the presence of microbubbles was a strict requirement for ultrasound-mediated gene-transfer events to occur in the 3D matrices. It was also clear, from both the data presented in this study and previous studies (Nomikou et al., 2012), that the biotinylated cationic microbubble provided advantage with respect to gene transfer, and it was suggested that this was due to the observation

direct contact between nucleic acid and target cells in the matrices. Based on these observations, if one employed a neutral microbubble in matrix formulations and these were dispensed into the wells of a 96-well plate, one might expect the microbubbles to float to the surface prior to complete gelation of the matrix (Figure 3A, left). In effect, an uneven distribution of transfected cells would be obtained in such matrices, with the most transfected population of cells inhabiting the upper sections of the matrix because of microbubble floatation prior to gelation. If, on the other hand, the biotinylated cationic microbubble was employed, then direct interactions would occur between the microbubble, DNA and the target cells, and a more even distribution of transfected cells would exist within matrices, because electrostatic interactions would preclude separation of the target cells and the microbubbles (Figure 3A, right). In order to test this hypothesis and confirm advantage associated with the use of the biotinylated cationic microbubble for ultrasound-mediated gene transfer in 3D matrices, it was decided to compare the distribution of luciferase expression down through the matrix following ultrasound-mediated gene transfer in the presence of both microbubbles. In order to do this, we exploited the fact that the emission of photons during the luciferase-based that these microbubbles were capable of mediating bioluminescent assay was dependent on top-to-bottom diffusion of the luciferin solution through the 3D matrices. In effect, it was decided to examine the time dependence of bioluminescent signal production for 40 min following the addition of the substrate to the matrix-containing wells, in which either the neutral or biotinylated cationic microbubbles were employed for ultrasound-mediated gene transfer. Essentially, cell-, microbubble(neutral and biotinylated cationic) and DNA-containing matrices were treated with ultrasound and, 24 h after treatment, luciferin was added to the top of matrices in each well and the emission of bioluminescence was recorded every 5 min for a 40 min period. The results are presented in Figure 3B and demonstrate that, while luciferin diffused through the

matrix, the emission of bioluminescent signal increased continuously during the first 40 min when biotinylated cationic microbubbles were used for ultrasound-mediated gene transfer. However, where neutral microbubbles were employed for ultrasound-mediated gene transfer, the bioluminescent signal reached a maximum within 20 min. These observations are consistent with our hypothesis. If the neutral microbubbles were floating to the top prior to or during gelation, then one would expect the bioluminescent signal to develop to a maximum early in the assay, because most of the transfected cells would reside in the upper regions of the matrix (Figure 3A, left). The data obtained when the biotinylated cationic microbubble was used for ultrasound-mediated gene transfer, however, suggested that cells embedded in the matrix deeper in the gel had been transfected, because the bioluminescent signal continued to increase as the substrate diffused down through the matrix, and we suggest that this was the result of the cationic microbubble being bound to target cells, as shown in Figure 3A (right). In confirming our hypothesis, these results highlight the benefits afforded by the use of the biotinylated cationic microbubble in 3D matrix formulations, both from the perspective of enhancing ultrasound-mediated gene transfer and from affording a more even distribution of gene transfer in those matrices.

3.4. The effect of collagen on ultrasound-mediated gene transfer in fibrin-based matrices

Fibrin-based biomaterials have found increasing use in the field of tissue-engineering applications (Zhang et al., 2012; Yasuda et al., 2010). Fibrin possesses a major advantage for such applications, because it rapidly forms flexible or rigid matrices from injectable liquid formulations. Our choice of fibrin as a matrix was driven by its injectable nature and the ability to control gelation time without adverse separation of the components necessary to promote ultrasound-mediated gene transfer, as described in the previous section. In our initial studies we employed collagen in the fibrin-based matrices because it has previously been shown to provide firm hydrogels that have

improved properties for tissue-regeneration applications (Schneider et al., 2010; Feng et al., 2010). These properties include increased permeability, great tensile strength and smooth microgeometry. Here, it was of interest to determine whether or not collagen was playing any role in facilitating ultrasound-mediated gene transfer within the fibrin-based matrices, or whether its presence simply provided structural benefit. To this end, fibrin-based matrices, prepared in the presence and absence of collagen, were treated using optimal ultrasound conditions in the presence of optimal concentrations of biotinylated cationic microbubbles and DNA. The results obtained from these experiments are shown in Figure 4 and, surprisingly, they clearly demonstrated a strict requirement for collagen in the matrix, since ultrasound-mediated gene transfer was approximately 25-fold lower in its absence.

Since these results suggested that collagen was playing some active role in the process, it was decided to determine whether or not the necessity for collagen was associated with differences in cell viability in matrices in the presence or absence of collagen. Growth of cells inoculated into matrices at different concentrations ($2-8 \times 10^4$ cells/matrix), in the presence or absence of collagen, was examined using the Fda-based assay. As shown in Figure 5A, growth rates were similar in both matrices. Similarities in cell growth in both matrices was further confirmed by direct counting of DAPI-stained cells in cryosections at 2 and 24 h after cell inoculation into both matrices. For example, when 6×10^4 cells were inoculated into matrices, the direct cell count in the fibrin-collagen sections after 24 h showed a 2.8-fold increase in cell number (Figure 5B). The equivalent cell number increase over this time period, and based on the Fda assay (Figure 5A), was calculated to be 2.3-fold. Similarly, when 6×10^4 cells were seeded in the fibrin matrices, the direct cell count showed a 2.0-fold increase in cell number, and this was comparable with the 1.9-fold increase

calculated from the Fda assay for this matrix. Even though two different methods were employed here to determine cell viability, both methods yielded similar data and were confirmatory of the observation that cell growth was similar in both the fibrin and fibrin–collagen matrices. On the basis of these observations, we suggest that the increase in gene expression observed in the collagen-containing matrices is not a result of enhanced cell growth in those matrices.

Histological analysis of the matrices was also performed in order to determine any morphological differences between the matrices in the presence and the absence of collagen. The Van Gieson's stain was used in order to detect any peculiarities with respect to collagen distribution within the fibrin–collagen matrices. Using this particular stain, nuclei stain black and collagen stains pink to red. As shown in Figure 6, the morphology of the matrices, in either the presence or absence of collagen, was similar. No obvious accumulations of collagen in or around individual cells were observed and this component was relatively evenly blended throughout the fibrin-based matrix. In addition to examining the morphology of the matrices, the ability of ultrasound energy to pass through these matrices was examined, using an ultrasound power meter. The measurements demonstrated that both matrix formulations, in either the presence or absence of collagen, transmit > 90% of the ultrasound energy at an ultrasound power density of 4 W/cm^2 (data not shown). However, it should be noted that the use of a power meter to assess ultrasound transmission is relatively crude, and even very small differences in ultrasound transmission efficiency may play a very significant role at the microscopic level, particularly with respect to the behaviour of microbubbles and the manner in which these reagents respond to ultrasound within the 3D matrix. The data presented thus far have demonstrated that gene transfer in 3D matrices can be achieved by the application of the sonoporation-based system described above. However, a considerable

amount of thrombin-containing CaCl_2 (50% v/v) was added to the mixture in order to form the fibrin-based hydrogels. It was thought that the presence of CaCl_2 , together with the phosphate in the buffers used in the mixture, may have led to the formation of calcium phosphate nanoparticulates, which can, in some cases, promote gene transfer (Keeney et al., 2010). In order to demonstrate that gene transfer successfully occurred as a result of sonoporation and not as a result of the presence of calcium phosphate in the fibrin-based matrices containing collagen, matrices were treated with ultrasound in the presence or absence of microbubbles. A third matrix was also established with the same plasmid and microbubble concentrations; however ultrasound treatment was omitted. The results shown in Figure 4 clearly demonstrate that gene transfer in the 3D matrices is facilitated exclusively by sonoporation, which requires both the presence of microbubbles and ultrasound treatment at the optimized conditions described above. The results also demonstrate that gene transfer is not related to the presence of Ca^{2+} in matrix formulations.

Although the precise mechanism by which the presence of collagen in fibrin-based matrices is essential for ultrasound-mediated gene transfer is as yet unknown, it is clear from the studies above that ultrasound-mediated gene transfer is possible in these 3D matrices. Since the matrix components can be formulated in suspension/solution, mixed immediately prior to administration, administered as a liquid and compatible with rapid gelation immediately post administration, the ultrasound-responsive system could be exploited in a wide variety of applications in the area of tissue regeneration. In comparative terms, the only technology currently available to enable any degree of extracorporeal control over gene transfer into matrix-entrapped stem cells, post administration, would be electroporation. Recently, electroporation was employed for gene transfer of cells in an implanted 3D matrix for the purposes of tissue regeneration (Kimelman-Bleich et al., 2011). However, this approach requires direct electrical contact with the target site

and involves some degree of invasion (insertion of needles, etc.). These requirements have placed limitations on the application of electroporation in tissue engineering, particularly for target sites that may be located deep within the body. In addition, the degree to which electrical pulses can afford spatially predictable site-specific gene transfer in different parts of an implanted matrix is constrained by impedance, resistance and conductivity variables within a matrix and by the inability to focus electroporative pulses to a single point in space (Davalos et al., 2004). On the other hand, ultrasound is recognized as a truly non-invasive stimulus for gene transfer (Nomikou and McHale, 2010). Results in the current study suggest that ultrasound in combination with microbubbles provide an ideal means of facilitating gene transfer to stem cells entrapped within a tissue-regeneration matrix. Such a system could be employed in order to extracorporeally control morphogenesis/differentiation of stem cell populations immobilized in a scaffold biomaterial, which is embedded deep within tissues. In considering the benefits afforded by the above-described system for the purposes of tissue regeneration, it is essential to appreciate the spatial and temporal control aspects of this platform. It is clear from the study that gene transfer would not have occurred in these matrices without the application of ultrasound in the presence of microbubbles. Since we can control the time at which ultrasound is applied, this affords temporal control of gene transfer, either for in vitro, ex vivo applications or potentially in a postsurgical environment. In terms of the latter, this provides the combined advantages of retaining the target cell population at the required site (e.g. in the cavity of a non-union fracture) and further allowing the target cell population to become accustomed to its new environment (Yasuda et al., 2010). Also, since hydrogel application and ultrasound treatment can be localized at a specific site, this system also facilitates controlling gene transfer spatially within a 3D matrix and within any give tissue. Essentially, the above-described system, employed with the appropriate stem cell

populations and nucleic acid constructs, has the potential to be exploited for non-invasive stimulation of gene transfer and expression at any time postimplantation of the tissue matrix formulation, and with a very considerable degree of spatial control. One aspect of our current work relates to optimizing this system for ultrasound-mediated gene transfer using bone morphogenic protein (BMP)-encoding DNA constructs for in vitro and in vivo osteogenesis in 3D matrices, and exploring the use of such a system in orthopaedic applications.

Acknowledgement

This work was funded by a EUROSTARS award (Project No. E5650-UGen), administered by both the Irish and Austrian Governments. The authors wish to gratefully acknowledge Dr. J. Barry at Baxter Innovations, Vienna, Austria for advice and expertise in relation to use of fibrin matrix components.

Conflict of interest

Dr N. Nomikou is head of R&D at Sonidel Ltd, Dublin, Ireland

References

Bouuaert CC, Chalmers RA. 2009; Gene therapy vectors: the prospects and potentials of the cut-and-paste transposons. *Genetica* 138(5): 473–484.

Bushman FD. 2007; Retroviral integration and human gene therapy. *J. Clin. Invest.* 117(8): 2083–2086.

Correa de Sampaio P, Auslaender D, Krubasik D, et al. 2012; A heterogeneous in vitro three-dimensional model of tumour-stroma interactions regulating sprouting angiogenesis. *PLoS One* 7: e30753, 1–14

Davalos RV, Otten DM, Mir LM, et al. 2004; Electrical impedance tomography for imaging tissue electroporation. *IEEE Trans Biomed Eng* 51: 761–767.

Feichtinger G, Redl H, van Griensven M. 2010; Fibrin as gene-activated matrix. In *Biological Adhesive Systems: from Nature to Technical and Medical Application*, von Byern J, Grunwald I (eds). Springer:, USA; 254–255.

Feng X, Shaker M, Clark R, et al. 2010; Fibrin and type I collagen 3-D matrix differentially regulate sprout angiogenesis of human dermal microvascular endothelial cells. *EJC Suppl* 8(5): 90–91.

Geiger F, Bertram H, Berger I, et al. 2005; Vascular endothelial growth factor gene-activated matrix (VEGF165-GAM) enhances osteogenesis and angiogenesis in large segmental bone defects. *J. Bone Miner. Res.* 20(11): 2028–2035.

Gonzalez AM, Berlanga O, Leadbeater WE, et al. 2009; The deployment of adenovirus-containing

gene activated matrices onto severed axons after central nervous system injury leads to transgene expression in target neuronal cell bodies. *J. Gene Med.* 11(8): 679–688.

Judo N, Okada K, Yamamoto K. 2009; Sonoporation by single-shot pulsed ultrasound with microbubbles adjacent to cells. *Biophys. J.* 96: 4866–4876.

Katagiri T, Komaki YA, Abe E, et al. 1994; Bone morphogenic protein-2 converts the differentiation pathway of C2C12 myoblasts into the osteoblast lineage. *J. Cell Biol.* 127: 1755–1766.

Keeney M, van den Beucken JJP, van der Kraan PM, et al. 2010; The ability of a collagen/calcium phosphate scaffold to act as its own vector for gene delivery and to promote bone formation via transfection with VEGF 165. *Biomaterials* 31 (10): 2893–2902.

Copyright © 2013 John Wiley & Sons, Ltd.

Keibl C, Fügl A, Zanoni G, et al. 2011; Human adipose derived stem cells reduce callus volume upon BMP-2 administration in bone regeneration. *Injury* 42(8): 814–820.

Kimelman-Bleich N, Pelled G, Zilberman Y, et al. 2011; Targeted gene-and-host progenitor cell therapy for nonunion bone fracture repair. *Mol. Ther.* 19(1): 53–59.

Kofron MD, Laurencin CT. 2006; Bone tissue engineering by gene delivery. *Adv. Drug Deliv. Rev.* 58: 555–576.

Lee MH, Kim YJ, Kim HJ, et al. 2003; BMP-2induced Runx2 expression is mediated by Dlx5 and TGF- β 1 opposes the BMP-2induced osteoblast differentiation by suppression of DLx5 expression. *J. Biol. Chem.* 280; 34387–34394.

Li YS, Davidson E, Reid CN, et al. 2009; Optimising ultrasound-mediated gene transfer (sonoporation) in vitro and prolonged expression of a transgene in vivo: potential applications for gene therapy of cancer. *Cancer Lett.* 273: 62–69.

Li YS, Reid CN, McHale AP. 2008; Enhancing ultrasound-mediated cell membrane permeabilisation (sonoporation) using a high frequency pulse regime and implications for ultrasound-aided cancer chemotherapy. *Cancer Lett.* 266(2): 156–162.

Liu H, Collins SF, Suggs LJ. 2006; Threedimensional culture for expansion and differentiation of mouse embryonic stem cells. *Biomaterials* 27(36): 6004–6014.

Mulder G, Tallis A, Marshall T, et al. 2009; Treatment of nonhealing diabetic foot ulcers with a platelet-derived growth factor gene-activated matrix (GAM501): results of a phase 1/2 trial. *Wound Repair Regen.* 17(6): 772–779.

Nakashima A, Katagiri T, Tamura M, 2005; Crosstalk between Wnt and bone morphogenic protein 2 (BMP-2) signalling in differentiation pathway of C2C12 myoblasts. *J. Biol. Chem.* 280; 37660–37668.

Nomikou N, McHale AP. 2010; Exploiting ultrasound-mediated effects in delivering targeted, site-specific cancer therapy. *Cancer Lett.* 296:133–143.

Nomikou N, Tiwari P, Trehan T, et al. 2012; Studies on neutral, cationic and biotinylated cationic microbubbles in enhancing ultrasound-mediated gene delivery in vitro and in vivo. *Acta Biomater.* 8(3): 1273–1280.

Osawa K, Okubo Y, Nakao K, et al. 2009; Osteoinduction by microbubble-enhanced

transcutaneous sonoporation of human bone morphogenetic protein-2. *J. Gene Med.* 11(7): 633–641. Park JS, Shim M, Shim SH, et al. 2011;

Chondrogenic potential of stem cells derived from amniotic fluid, adipose tissue, or bone marrow encapsulated in fibrin gels containing TGF- β 3. *Biomaterials* 32(32): 8139–8149.

Pérez RA, Won J, Knowles JC, et al. 2013; Naturally and synthetic smart composite biomaterials for tissue regeneration. *Adv. Drug Deliv. Rev.* <http://dx.doi.org/10.1016/j.addr.2012.03.009>.

Powell HM, Armour AD, Boyce ST. 2011; Fluorescein diacetate for determination of cell viability in 3D fibroblast–collagen– GAG constructs. *Mammalian cell viability: methods and protocols. Method Mol Biol* 740(13): 115–126.

Schillinger U, Wexel G, Hacker C, et al. 2008; A fibrin glue composition as carrier for nucleic acid vectors. *Pharm. Res.* 25(12): 2946–2962.

Schneider RK, Puellen A, Kramann R, et al. 2010; The osteogenic differentiation of adult bone marrow and perinatal umbilical mesenchymal stem cells and matrix remodelling in three-dimensional collagen scaffolds. *Biomaterials* 31(3): 467–480.

Suzuki R, Oda Y, Utoguchi N, et al. 2011; Progress in the development of ultrasound-mediated gene delivery systems utilizing nanoand microbubbles. *J Control Rel* 149: 36–41.

ter Haar G. 2007; Turning up the power: high intensity focused ultrasound (HIFU) for the treatment of cancer. *Ultrasound* 15: 73–77.

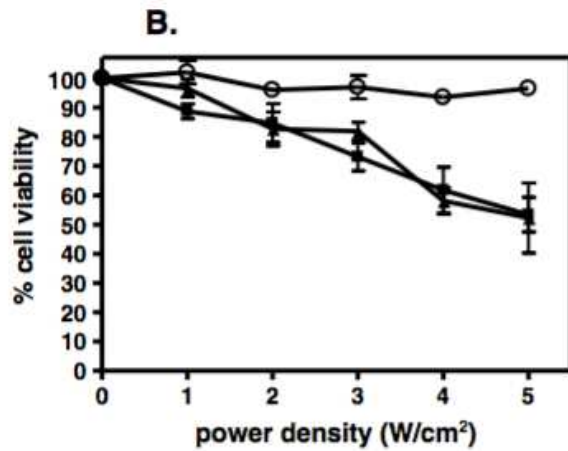
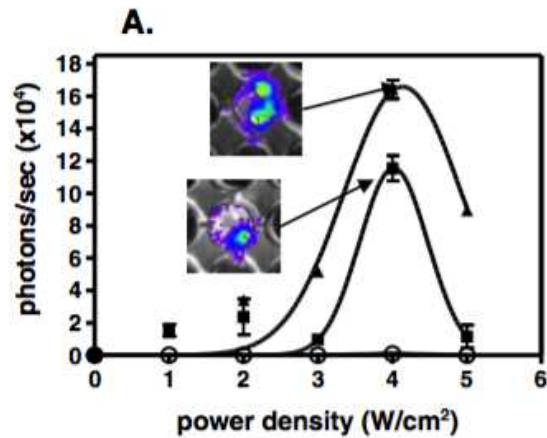
Wang X, Jin L, Ji S, et al. 2011; Hepatocytic differentiation of rhesus monkey embryonic stem cells promoted by collagen gels and growth factors. *Cell Biol. Int.* 35(8): 775–781.

Yasuda H, Kuroda S, Shichinohe H, et al. 2010; Effect of biodegradable fibrin scaffold on survival, migration, and differentiation of transplanted bone marrow stromal cells after cortical injury in rats. *J. Neurosurg.* 112(2): 336–344.

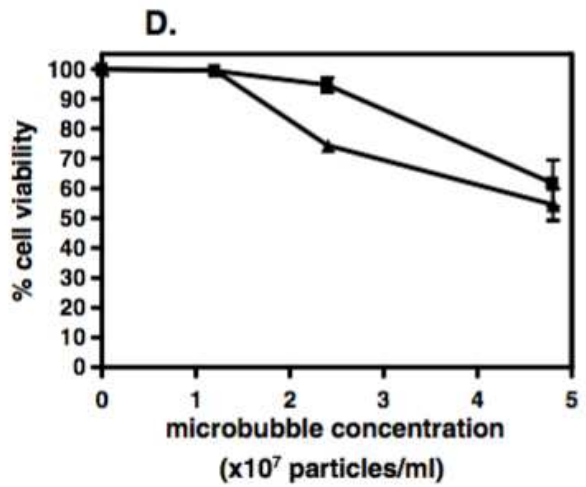
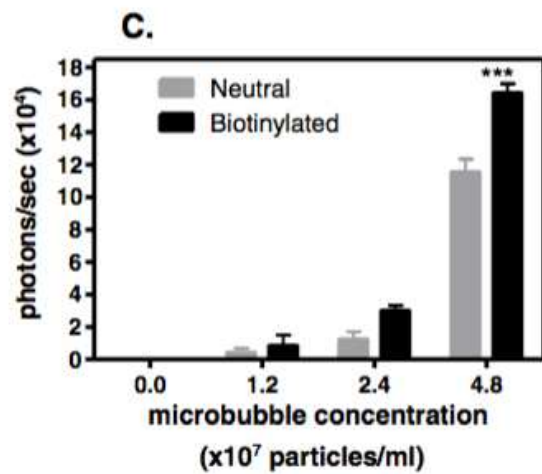
Zhang L, Wang P, Mei S, et al. 2012; In vivo alveolar bone regeneration by bone marrow stem cells/fibrin glue composition. *Arch. Oral Biol.* 57(3): 238–244.

Zhao M, Zhao Z, Koh JT, et al. 2005; Combinatorial gene therapy for bone regeneration: cooperative interactions between adenovirus vectors expressing bone morphogenetic proteins 2, 4, and 7. *J. Cell. Biochem.* 95: 1–16.

Ultrasound intensity



Microbubble concentration



DNA concentration

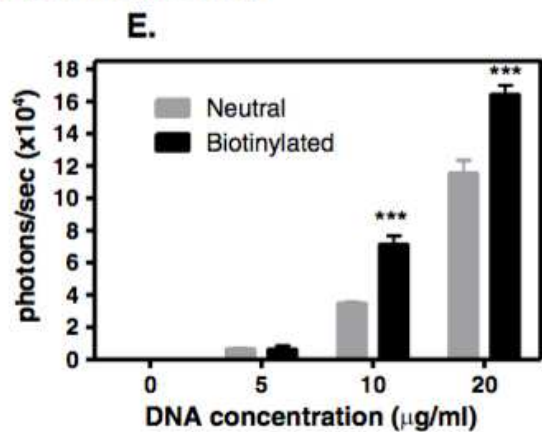


Figure 1: Parameters affecting the level of luciferase expression (A, C, E) and cell viability (B, D) in the presence of neutral (■) and biotinylated cationic microbubbles (▲) in the 3D fibrin–collagen matrices. In (A, B) a control

population of cells was treated with ul- trasound in the absence of microbubbles (○). Error bars represent SEM, where $n = 5$; *** $p < 0.001$ when all datasets were compared in the relevant panels.

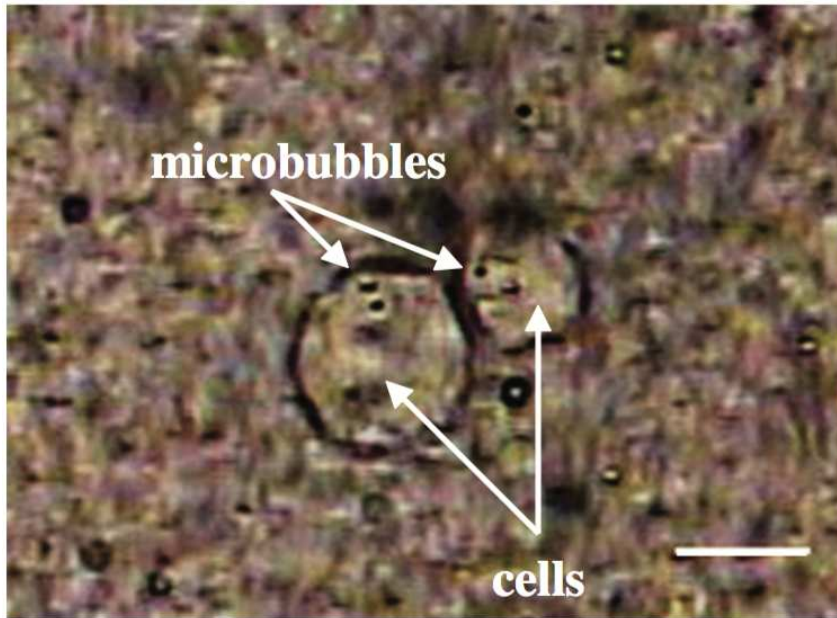


Figure 2: Photomicrograph showing the biotinylated cationic microbubbles attached on cells inside the fibrin-collagen-based 3D matrices; bar = 20 μm .

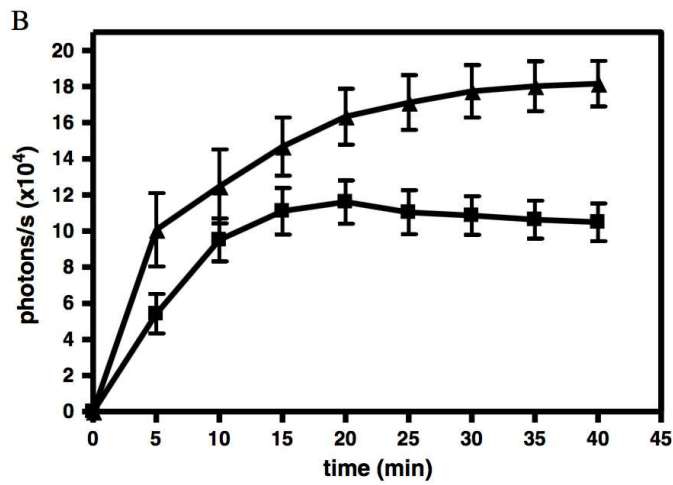
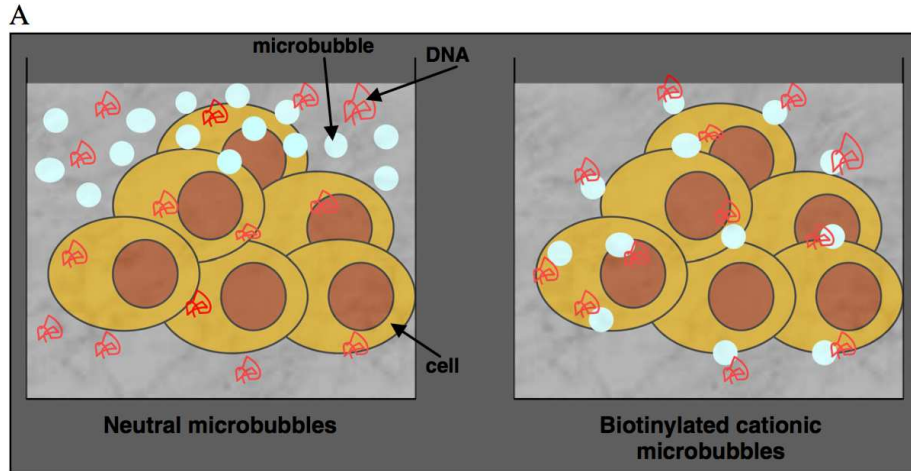


Figure 3: Hypothetical illustration of the component positions within the matrix prior to sonoporation (A) and bioluminescence during diffusion of luciferin through the fibrin–collagen matrices, treated in the presence of neutral (■) and biotinylated cationic microbubbles (▲) (B).

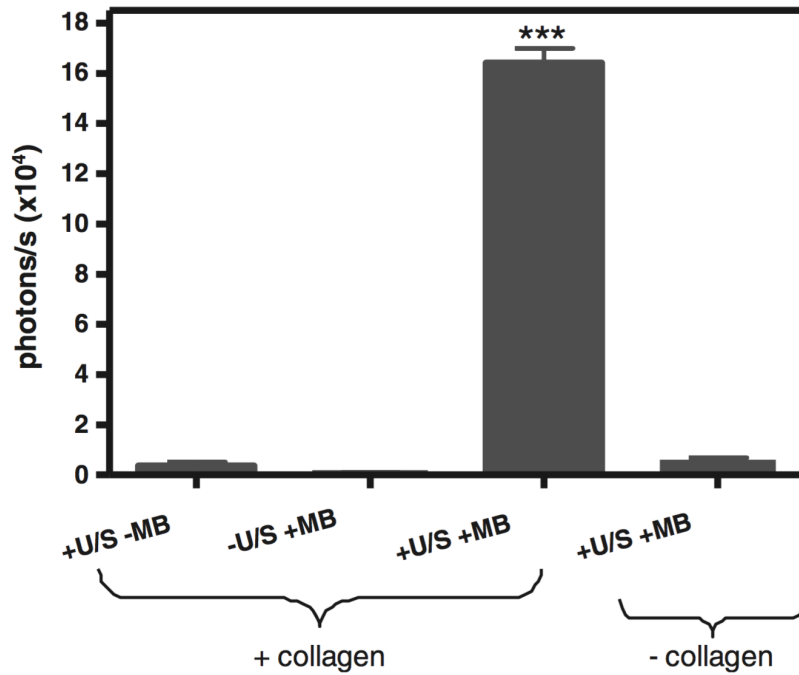


Figure 4: Luciferase expression in fibrin-matrices containing collagen (+ collagen) treated with ultrasound in the absence of the microbubbles (+U/S -MB); in the presence of microbubbles without ultrasound treatment (U/S + MB) and in the presence of microbubbles with ultrasound treatment (+U/S + MB). Luciferase expression was also examined in fibrin matrices without collagen (collagen) in the presence of microbubbles with ultrasound treatment (+U/S + MB). In the interests of clarity, other controls in the absence of collagen included treatment with ultrasound in the absence of microbubbles and treatment with microbubbles in the absence of ultrasound. In the latter two controls no bioluminescent signal was observed. Error bars represent SEM where n=5; ***p<0.001 when +U/S+MB for the +collagen group was compared with all other data groups in the experiment.

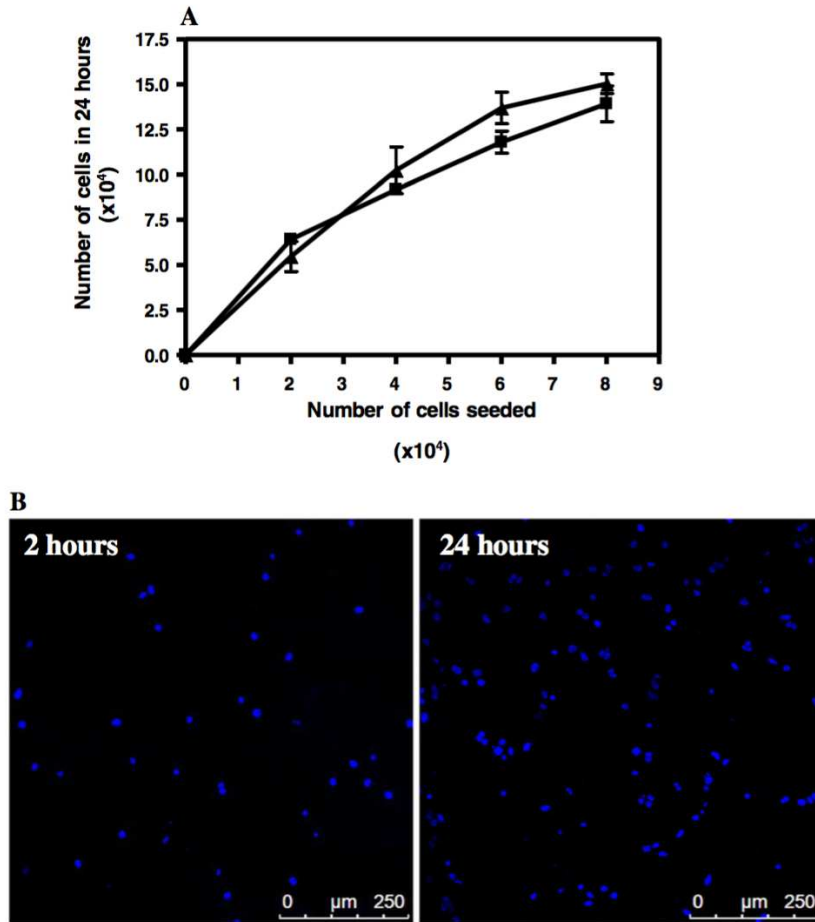


Figure 5: Growth curve of cells seeded in fibrin (■) and fibrin-collagen (▲)-based matrices (A) and representative confocal photomicrographs showing DAPI-stained nuclei of cells, 2 and 24 h after incorporation into fibrin-collagen matrices (B); bar = 250 μ m.

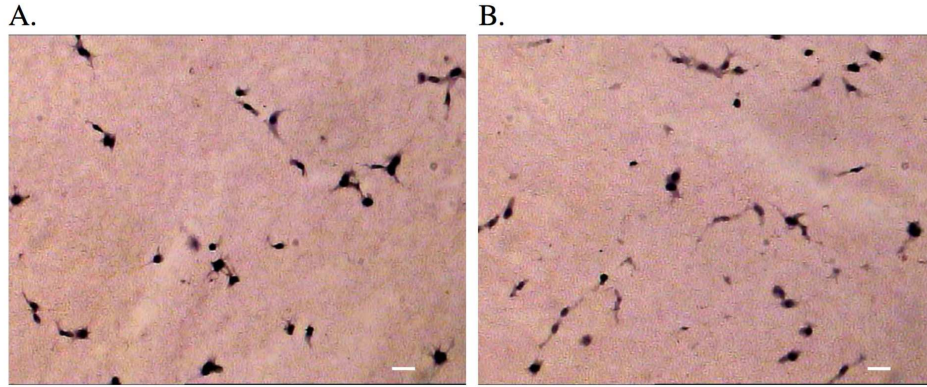


Figure 6: Representative photomicrographs of the Weigert's iron haematoxylin/Van Gieson-stained sections of fibrin (A) and fibrin–collagen (B) matrices, incubated for 24 h; bar = 20 μ m.